HIGH RESOLUTION RESULTS AND SCALABILITY OF NUMERICAL MODELING OF WIND FLOW AT WHITE SANDS MISSILE RANGE

Patrick A. Haines*
Computational & Information Science Directorate, Army Research Laboratory
White Sands Missile Range, NM USA

David J. Grove
Computational & Information Science Directorate, Army Research Laboratory
Aberdeen Proving Grounds, MD USA

Professor Wen-Yih Sun
Department of Earth & Atmospheric Science, Purdue University
West Lafayette, IN USA

Professor Wu-Ron Hsu
Department of Atmospheric Science, National Taiwan University
Taipei, Taiwan

ABSTRACT

The NTU/ Purdue nonhydrostatic numerical model has been developed over the last 6 years to predict atmospheric motions and conditions for both the mesoscale (200 m to 200 km) and large scale turbulence scale (20 m to 200 m). It is a fully explicit, compressible three-dimensional code and has compared quite to a wide variety of known analytical solution or observed situations including the Boulder Wind Storm, nonhydrostatic and hydrostatic mountain waves for flow over an isolated mountain and a 2-dimensional mountain barrier, and buoyant bubble.

The model has application to FCS requirements for providing fine scale weather information for small unit operations in near real-time. It will enable us to study and better understand the problems of diagnosing and predicting atmospheric flow and conditions in real terrain. It is also designed and being applied to simulate larger turbulent eddies particularly in stable atmospheric boundary layers which are important for night operations. Large scale turbulence is a key to accounting for small scale turbulence that affects electromagnetic and acoustic propagation and governs local diffusion.

This paper considers both idealized and real terrain simulations in which the model was applied at high resolution (Δx, Δy of 500 m to 1 km) to the Organ, San Andres and Franklin Mountains region on and near the White Sands Missile Range (WSMR) in New Mexico. We used DTED level 1 terrain data (3 arc second resolution) to generate the model's terrain fields.

1. INTRODUCTION

Air flowing over and around topographic obstacles is disturbed in a wide variety of ways including lee and mountain waves, rotor flows, hydraulic jumps, lee vortices, and so on. The nature of the disturbance seems to depend on the upstream atmospheric stratification and wind flow, the depth, width and complexity of the terrain obstacle, and whether the obstacle is 2-dimensional or 3-dimensional. In this study, we strive to better understand the resulting disturbances and limitations to their prediction through both observations and numerical modeling. Numerical simulation on idealized terrain is useful because analytical results are available to validate a numerical model's results. In addition, results over idealized but analogous terrain using the actual wind and temperature sounding for well observed cases further explores a numerical model's capability. Nevertheless, it is essential to apply a numerical model on real terrain for a variety of actual weather conditions to reveal its forecast capability. To do this, we have used the data and terrain on the White Sands Missile Range which includes the Organ, San Andres and Franklin mountains of southern New Mexico and western Texas and the 3-dimenionsal version of the nonhydrostatic Purdue/ National Taiwan University model hereinafter referred to as the Purdue/NTU model.

Topographic effects on the weather are important considerations for military operations. The important phenomena include strong winds near the ground, pronounced turbulence near the ground and aloft, production of copious amounts of dust and other obscurants, and dominate the local and regional diffusion conditions.

Although the Organ mountains alone constitute a

Report Documentation Page

Form Approved
OMB No. 0704-0188

1. REPORT DATE	2. REPORT TYPE	3. DATES COVERED
00 DEC 2004	**N/A**	**-**

4. TITLE AND SUBTITLE	5a. CONTRACT NUMBER
High Resolution Results And Scalability Of Numerical Modeling Of Wind Flow At White Sands Missile Range	5b. GRANT NUMBER
	5c. PROGRAM ELEMENT NUMBER
6. AUTHOR(S)	5d. PROJECT NUMBER
	5e. TASK NUMBER
	5f. WORK UNIT NUMBER
7. PERFORMING ORGANIZATION NAME(S) AND ADDRESS(ES) **Computational & Information Science Directorate, Army Research Laboratory White Sands Missile Range, NM USA; Computational & Information Science Directorate, Army Research Laboratory Aberdeen Proving Grounds, MD USA**	8. PERFORMING ORGANIZATION REPORT NUMBER
9. SPONSORING/MONITORING AGENCY NAME(S) AND ADDRESS(ES)	10. SPONSOR/MONITOR'S ACRONYM(S)
	11. SPONSOR/MONITOR'S REPORT NUMBER(S)

12. DISTRIBUTION/AVAILABILITY STATEMENT
Approved for public release, distribution unlimited

13. SUPPLEMENTARY NOTES
See also ADM001736, Proceedings for the Army Science Conference (24th) Held on 29 November - 2 December 2005 in Orlando, Florida. , The original document contains color images.

14. ABSTRACT

15. SUBJECT TERMS

16. SECURITY CLASSIFICATION OF:			17. LIMITATION OF ABSTRACT	18. NUMBER OF PAGES	19a. NAME OF RESPONSIBLE PERSON
a. REPORT	b. ABSTRACT	c. THIS PAGE			
unclassified	**unclassified**	**unclassified**	**UU**	**8**	

fairly complex terrain three-dimensional obstacle, they are embedded within the San Andres/ Franklin mountain chain which extends from El Paso in the south over 100 miles north. Thus, depending on the situation, the weather phenomena induced near the Organ mountains may be primarily two or three dimensional in character, or both, making WSMR wind flows particularly diverse and numerically challenging.

The White Sands Missile Range lies astride and adjacent to the Organ and San Andres mountains. Because it is a major test center, it has a mesoscale surface observation network, the Surface Automated Measurement System (SAMS) consisting of twenty-one instrumented 10 m towers making continuous surface measurements at WSMR. The majority of the stations are located on the northern part of the range, so that the number of SAMS is somewhat limited (five stations) on southern part of WSMR near the Organ mountains. To augment the number of SAMS near the Organs, the Army Research Laboratory set up 5 instrumented 10 m towers. ARL is also very much indebted to Mr. Robert Cox proprietor of the Cox Ranch who kindly allowed the installation of two ARL towers on the Cox Ranch in close proximity to the Organ mountains. In addition to these surface measurements, ARL collected a large amount of upper air and wind profiling radar soundings made at WSMR and Santa Teresa NM (El Paso), remote automated weather stations (RAWS) and other local weather network observations from January into March 2004.

2. NUMERICAL MODEL

The numerical model used in this study explicitly solves the fully compressible nonhydrostatic system of equations (Hsu and Sun, 2001) and builds on the proven success of a preceding hydrostatic numerical model (Chern, 1994, Sun et al. 1991, Sun and Chern, 1993, Haines et al., 1997). Such an approach may seem to be inefficient; however, it is simple, saves memory and is accurate for high frequency waves. The fully explicit system solution also gives a good comparison basis for the implementation of semi-implicit or other more time efficient schemes to ensure their accuracy. Last, but by no means least, an explicit algorithm is especially amenable to parallel computing.

The model uses a forward-backward scheme for sound and gravity waves. As such, values at the new calculation time immediately replace those of the preceding model calculation time during the calculation so that only one array is required. Therefore, this scheme requires only 50% of the memory space used by the centered finite difference schemes (needs current and old values in memory to calculate the new value) used in many numerical models. This scheme is also neutral with respect to linear sound and internal gravity waves, and produces no computational mode. This later attribute obviates the need to use a time filter. The intention of doing things in this way is to impose a minimum of artificial smoothing in order to obtain a more accurate solution.

The compressible set of equations admits fast sound waves necessitating a small time step for their solution. The consequences of the small time step are mitigated through use of the time-splitting technique (Gadd, 1978) in which the time integration is split into three stages; the corresponding time steps depend on the physical time scale of the calculated terms. The three time stages involve advection, sound and other fast waves and diffusion.

3. NUMERICAL SIMULATIONS

3.1 Two-dimensional Boulder wind-storm

On January 11, 1972, a severe down-slope wind storm occurred in Boulder, Colorado and along the Colorado Front Range (CFR). These storms occur occasionally along the there, but this day's storm is especially noteworthy because a research aircraft was able to document many facets of the wind storm that occurred on this day from the surface to the stratosphere.

To simulate this case, the model was set up two-dimensionally with its vertical grid spacing set to 400 m, and its horizontal resolution to 2 km. The model domain extends in the west to east direction for 220 km and vertically from the ground surface to 24 km. An idealized representation of a cross-section through the CFR was constructed using a witch of Agnesi curve

$$z_s(x) = h/(1 + x^2/a^2) \qquad (1)$$

where h = 2 km and a = 10 km; these are typical values for the CFR (Doyle et al., 2000). Beginning with an initial condition of the Grande Junction, Colorado sounding for 1200 UCT on 11 January 1972, the model is integrated for 4 hr or longer. The simulation at 4.5 hr will be discussed here. Simulations were done for a free-slip and no-slip surfaces with and without the Coriolis force and are presented in Figs. 1-5. With no Coriolis force, Figure 1 shows that the x-component wind on the lee of the mountains reaches 70 m s^{-1} or more for a free slip surface condition. Meanwhile, for this surface condition, the hydraulic jump moves eastward with time (see also Fig. 5). That the Coriolis force does not cause any significant differences for a free-slip surface, is

shown in Fig. 2 which is quite similar to Fig. 1. As shown in both figures, turbulence and gravity waves coexist in the lower atmosphere as well as in the stratosphere. For flow over a no-slip surface, however, the Coriolis force enhances the x-component wind on the lee considerably going from less than the 35 m s^{-1} shown in Fig. 3 to more than 50 m s^{-1} shown in Fig. 4 below. The latter value is comparable to the winds observed in Boulder on January 11, 1972. It is also notable that the position of the hydraulic jump remains stationary with time for the no-slip surface, as shown in Fig. 5. Train waves also developed on the lee side for the no-slip surface. Therefore, the results show that both surface viscosity and the Coriolis force are very important in a downslope wind storm. The influence of the Coriolis force was not addressed in previous studies of the Boulder wind storm. Some of these results were previously presented in Sun and Hsu (2003, 2004).

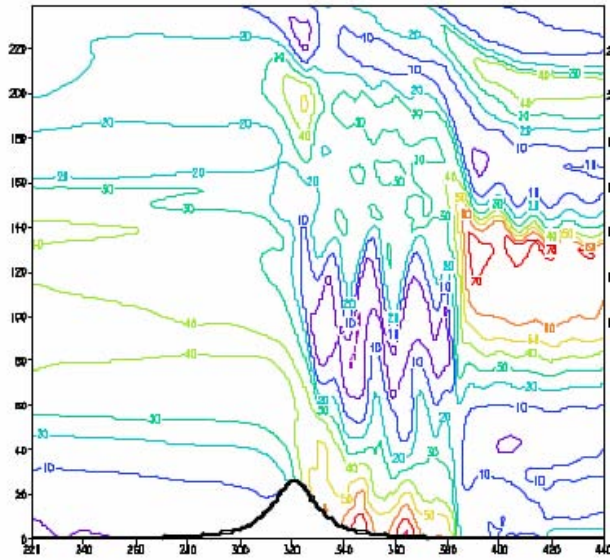

Fig. 1: Numerical simulation of Boulder Windstorm over a free-slip surface without Coriolis force at 25 N after 4.5 hr integration with a mountain height of 2 km. The vertical grid interval is 70m and horizontal grid space is 2 km. The x-component wind is shown and the hydraulic jump propagates away from the mountain with time.

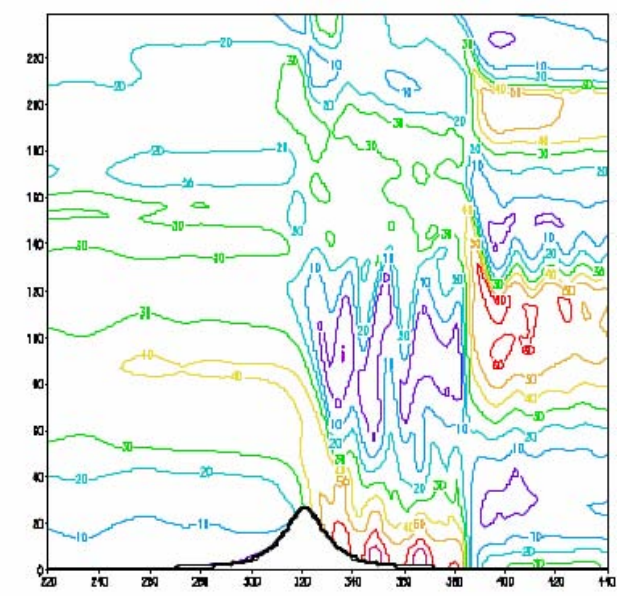

Fig. 2: Numerical simulation of the Boulder Windstorm over a free-slip surface with Coriolis force at 25 N after a 4.5 hr integration with mountain height of 2 km. The vertical grid interval is 70 m and horizontal grid space is 2 km. The x-component wind is shown. The hydraulic jump propagates away from mountain with time (similar to Fig. 1).

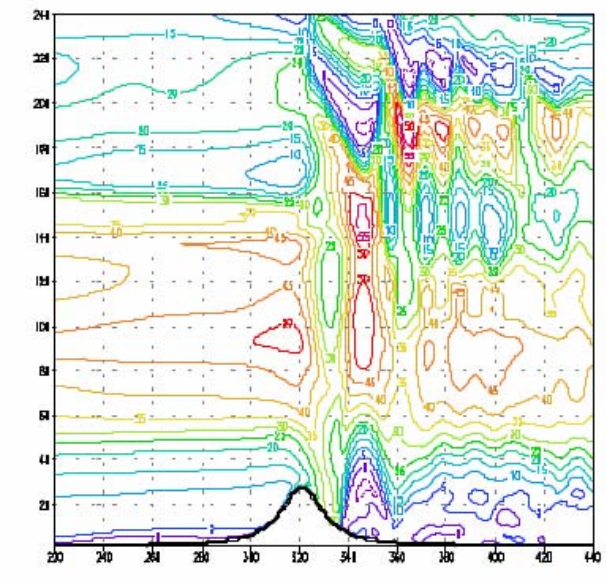

Fig. 3: Numerical simulation of Boulder Windstorm over a no-slip surface without Coriolis force at 25N after 4.5 hr integration with a mountain height of 2 km. The vertical grid interval is 70 m and horizontal grid space is

2 km. The x-component wind is shown and the hydraulic jump remains stationary.

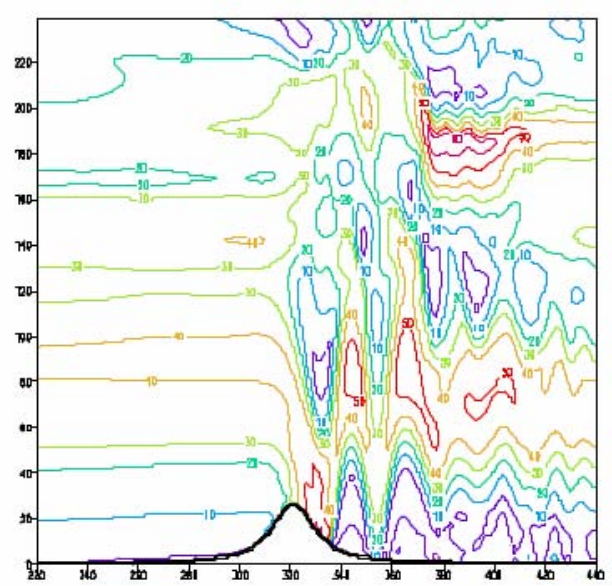

Fig. 4: Numerical simulations of the Boulder storm over a no-slip surface with Coriolis force at 25N after 4.5 hr integration with a mountain height of 2 km. The vertical grid interval is 70 m and horizontal grid space is 2 km. The x-component wind is shown and the hydraulic jump remains stationary, but both the horizontal wind which reaches 55 m s^{-1} near the surface and the vertical velocity which reaches 30 m s^{-1} are much stronger than for the no coriolis force results shown in Fig. 3.

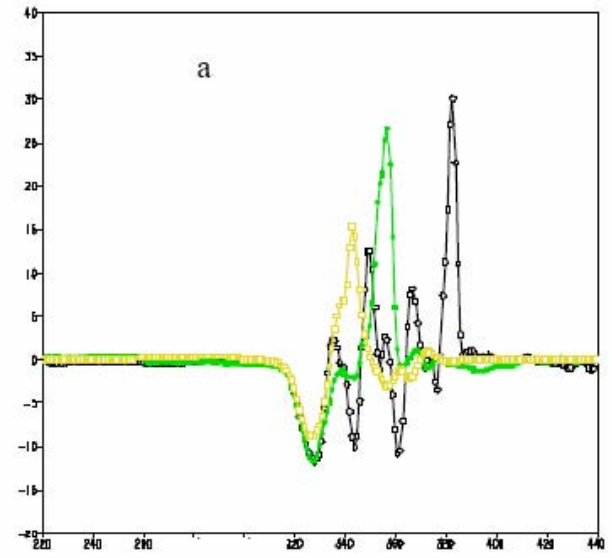

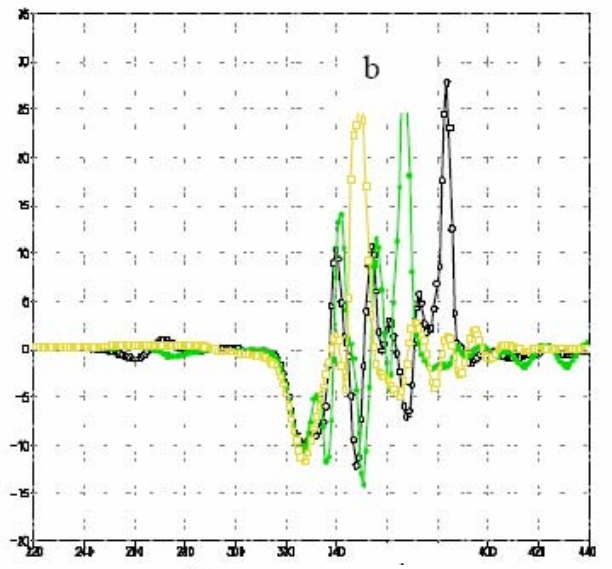

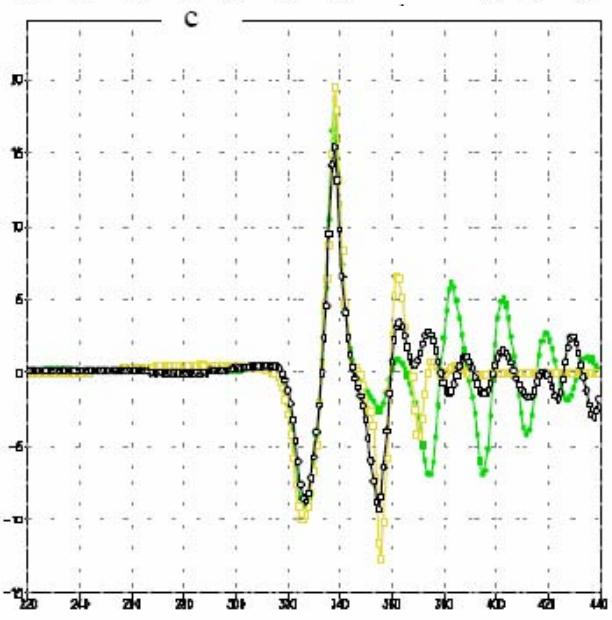

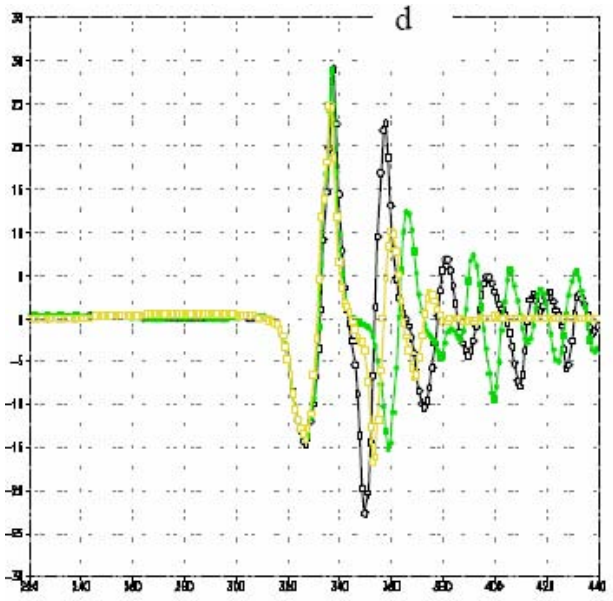

Fig. 5: Vertical velocity as a function of time along the x-axis (dx=2 km) at z=350 m at t=1.5 hr (yellow), t=3h (green), and t=4hr (black) for (a) free-slip surface without Coriolis force, (b) free-slip surface with Coriolis force, (c) no-slip surface without Coriolis force, and (d) no-slip surface with Coriolis force. (The hydraulic jump moves with time on free-slip surface (in a & b); but is stationary for a no-slip surface (in c & d), large-amplitude train waves also can be seen in c & d.

3.2 (b) Blocking effects by the terrain at WSMR

The blocking effects of mountains on air flow have been studied for years. However, most studies have been conducted with either an idealized mountain as above in **3.1 (a)**, or for synoptic-mesoscale systems due to the difficulty in collecting commensurately scaled observational data or even developing a reliable forecasting model. It has also been difficult to have enough computing resources to work on this problem three-dimensionally at high resolution until very recently. The results show that the high resolution Purdue/ NTU model is capable of reproducing the details of the flow in very pronounced terrain such as the Organ Mountains in the White Sands Missile Range under different prevailing winds. The domain used for the results shown here consisted of 100x100x60 grids with dx=dy=2 km and dz=300 m. The real terrain height is applied at the surface. We used four different prevailing winds:
(a) a 10 m s^{-1} westerly wind; (b) a 5 m s^{-1} southwesterly wind; (c) a 5 m s^{-1} westerly wind; and (d) the observed wind profile for the Boulder windstorm.

Because the blocking effect becomes more pronounced when the Froude number is less than 0.5 (Fr=U/NH; U is the prevailing wind, H is the height of the mountain, and N is Brunt-Väisällä frequency), we will present the results simulated from a 5 m s^{-1} westerly or southwesterly prevailing wind only. Figure 6 shows the simulated surface wind vector (a) and streamline (b) after 4-hr integration for an initial 5 m s^{-1} southwesterly wind.

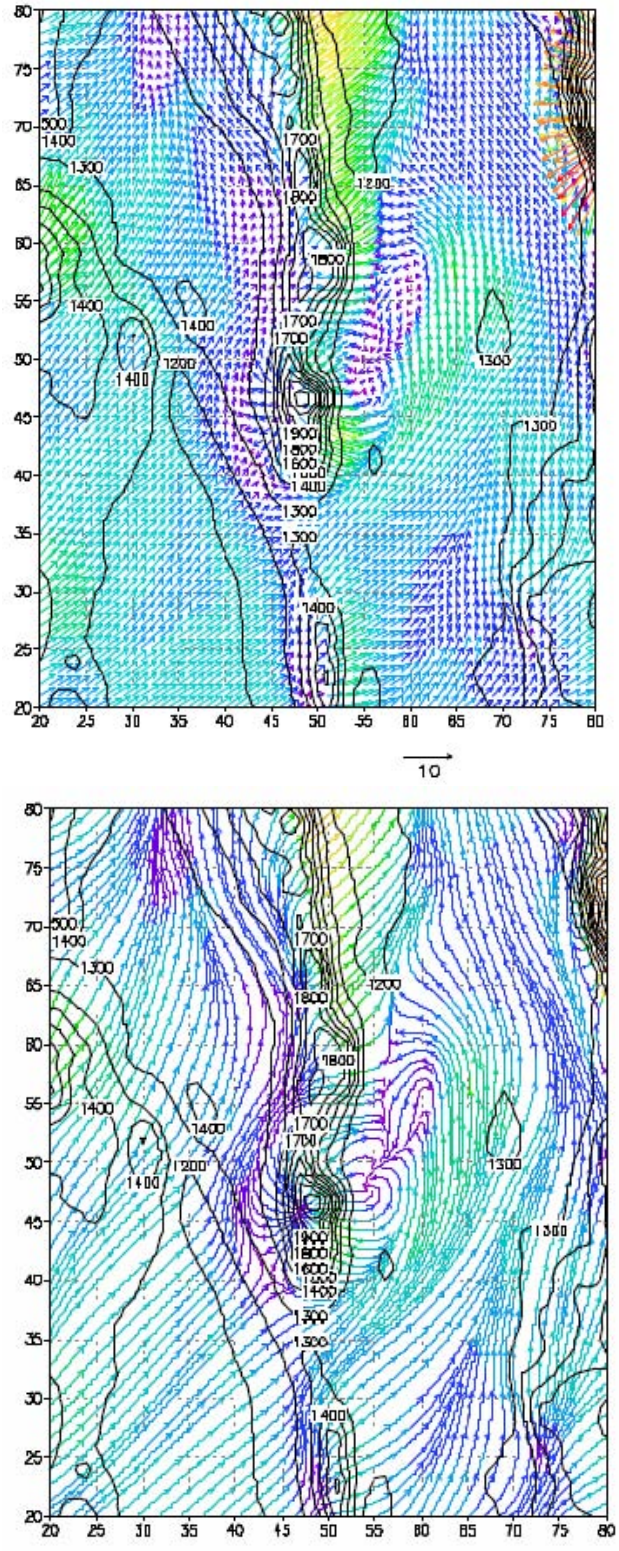

Top: 6 (a); Bottom: 6 (b)

Fig. 6: Model simulation of the surface wind vector (a) and streamline (b) over White Sands after a 4-hr integration, (with dx=dy=2 km, and dz=300m). Terrain height is indicated by the black contours (in m). The initial wind is 5 m s^{-1} coming from the southwest. Blocking by the mountain range produces counter-gradient flow on the upwind slope, and a lee-vortex and strong downslope winds on lee side. The wind direction also changes from southwesterly to southerly wind on both sides of mountain range near the northern part of the domain. A strong westerly wind also shows up at the valley (at x=50, y=52).

The black contours indicate the terrain height. We can see that the surface wind is blocked by the Organ Mountains and produces a counter-gradient flow on the windward side (near x=45, y=45), a strong wind at San Augustine Pass (near x =50 and y=52), and a lee vortex (at x=50-65, and y=40-60), as well as a strong downslope wind on the lee side, all of which are also clearly shown in the surface streamlines.

Blocking is still quite prominent in the wind vector shown at z =1.8 (Fig.7a), as well as the streamline and temperature field (Fig. 7b). Figure 7b shows that warming (warm color) on the lee side of Mountain ranges corresponds to a strong subsidence there with a cooling (blue color) on the wind ward side.

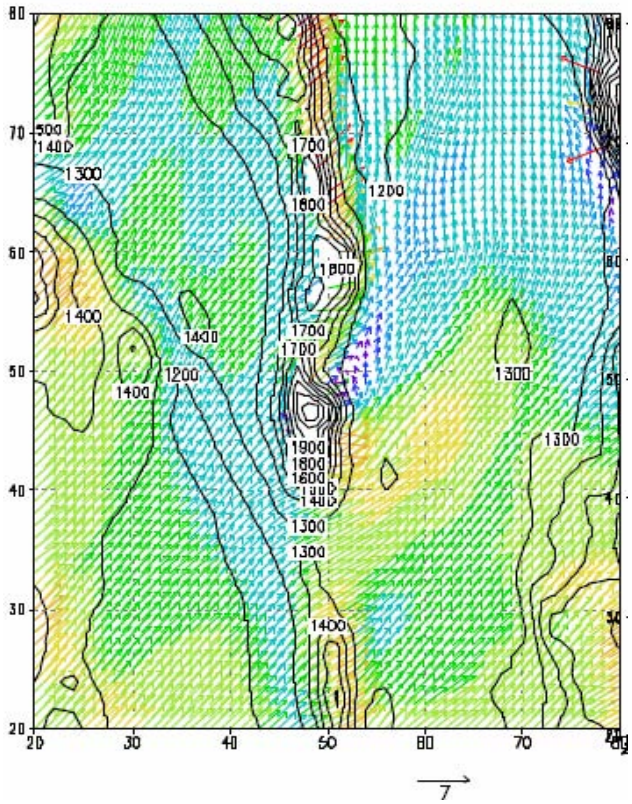

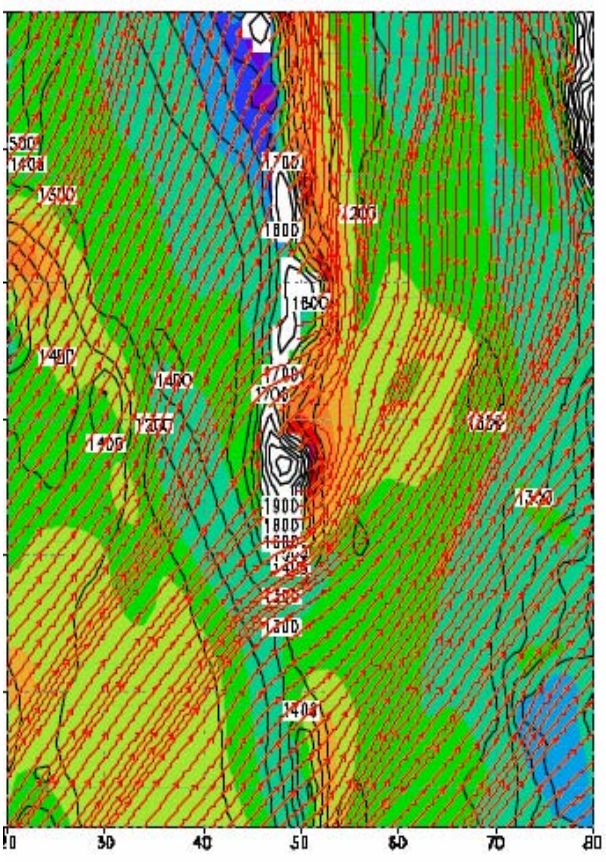

Fig. 7: Wind vector (left) and streamline (above) at height=1.8 km, showing that blocking by the mountain range is not as severe as at the surface, although we still see a small lee vortex on the lee side at x=53, and y=48, and a southerly wind in the northeastern region. Streamlines (red lines) and virtual potential temperature (indicated by background shaded colors) at z=1.8km, warm color (red) indicates subsidence warming on the lee-side, and cold (blue) color adiabatic cooling on the windward side of the mountain. The height of the terrain is indicated by black contours (in m). Mountain waves are clearly evident in these simulations but cannot be shown here due to limitations of space.

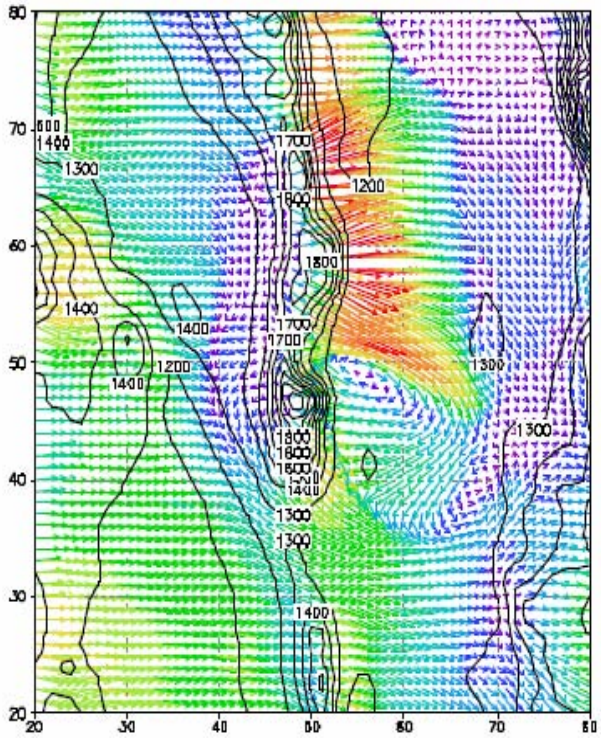

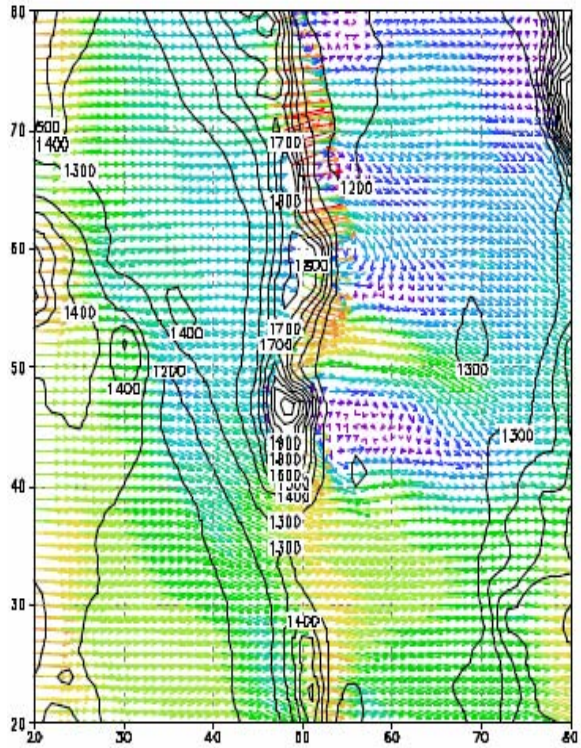

With a 5 m s^{-1} westerly wind, the blocking effect becomes more pronounced. We can see that vortices develop near the surface and extend to z=1.8 km (the height near mountain top) downwind of the Mountain Range, as shown in surface velocity field above in (Fig 8a), the wind field at 1.8 km (Fig. 8b) as well as the streamline and virtual potential temperature field at z =1.8 km (Fig. 8c) that is almost perpendicular to the prevailing wind. The streamline (Fig. 11) along the north-south cross section is very complicated, because of the formation of secondary circulation related to mountain waves (see the vertical line at x=50 in 14) in the y-z plane. They are also related to the vortices forming just behind the mountain range, as shown in Figs. 8.

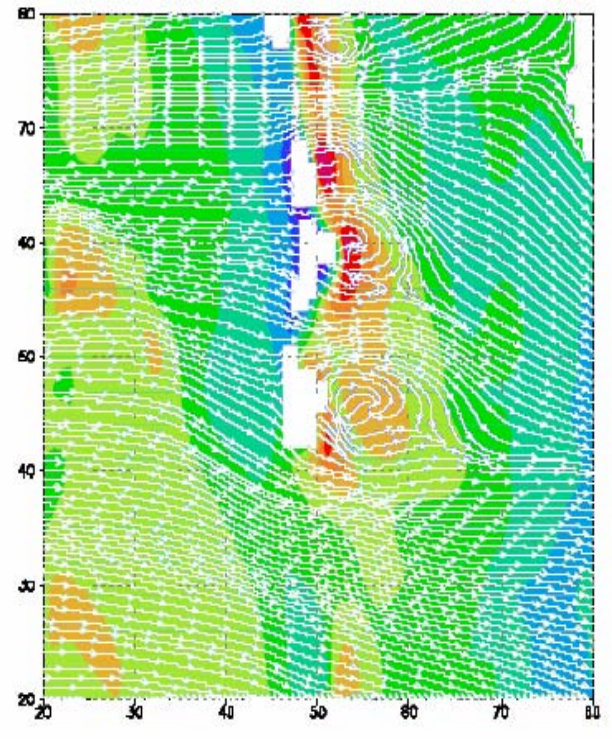

Fig 8: (a) Model simulation of the surface wind vector, (top); (b) wind at 1.8km (top right), and (c) stream line at 1.8 km (right) of the x-component velocity (shaded color and color lines) and potential temperature (white contours) along y=50 in White Sands after 4-hr integration, (with dx=dy=2 km, and dz=300 m). Terrain height is indicated by black contours (in m) or white blank. The initial wind is 5 m s^{-1} coming from the west.

The blocking effects of the WSMR terrain, particularly in the lee of the Organ Mountains have been shown in SAMS and other data (Grove and Haines, 2002). Grove and Haines noted that the wind flow shown

by the SAMS stations was consistent with formation of a lee vortex; however, the number of SAMS stations near the Organ Mountains is limited, and additional measurements would be required to fully reveal the actual flow. The kind of blocking seen in the numerical results also showed up in the meso-gamma experiment results for westerly and south-westerly flow cases in which the Froude Number was less than 0.5. During the meso-gamma experiment, hydraulic jumps in the lee of mountains are also revealed by analysis of meso gamma and SAMS pressure observations qualitatively similar to the numerical models' hydraulic jumps. The model was initialized with the El Paso (Santa Teresa, NM) sounding.

CONCLUSIONS

The Purdue/ NTU model was applied to both idealized and real terrain cases. The idealized case was the Boulder Wind Storm in which an idealized two-dimensional terrain cross-section was used. The model results are quite similar to observations made by an instrumented aircraft which documented the January 11, 1972 Wind Storm in some detail. Imposing a free-slip condition and the Coriolis force resulted in significant changes in the model results compared to free-slip conditions with no Coriolis force. The result with the Coriolis force is new and requires further study.

The model was also applied to some wind conditions on the WSMR terrain. With a Froude number of less than 0.5, the model shows that the terrain cause pronounced blocking along with formation of a lee vortex. The model flows are consistent with local WSMR surface flows observed fro these kinds of conditions.

Much additional work for higher Froude number conditions remains to be done. It is expected that the copious data collected during the Meso-Gamma experiment will prove very useful in this regard.

REFERENCES

Chern. J-D., (August, 1994) Numerical simulation of cyclogenesis over the western United States. Ph.D. thesis, Purdue University, W. Laf. IN. 178 pp.

Doyle et al. 2000: An intercomparison of model-predicted wave breaking for the 11 January 1972 Boulder windstorm. *Mon. Wea. Rev*., **128**, 901-914.

Gadd, A. J., 1978: A split explicit integration scheme for numerical weather prediction. *Quart. J. Roy. Met. Soc*., **104**, 569-582.

Grove, D. J., and P. A. Haines, 2002: Fine scale numerical prediction of atmospheric flow in complex terrain. 2002 DRI Report, US Army Research Laboratory, Adelphi, MD.

Haines, P. A., J. D. Chern. and W. Y. Sun, 1997: Numerical simulation of the Valentine's Day storm during WISP 1990. *Tellus*, **49A**. 595-61Õ.

Hsu, W, R., and W. Y. Sun, 2001: A time-split, forward-backward numerical model for solving a nonhydrostatic and compressible system of equations. *Tellus*, **53A** , 279-299.

Sun, W. Y., J. D. Chern, C.C. Wu, and W. R. Hsu. 1991: Numerical simulation of mesoscale circulation in Taiwan and surrounding area. *Mon. Wea. Rev.*, **119**, 2558-2573.

Sun, W. Y., and J. D. Chern, 1993: Diurnal variation of lee-vortexes in Taiwan and surrounding area. *J. Atmos. Sci.* **50**, 3404-3430.

Sun, W. -Y., and J.-D. Chern, 1994: Numerical Experiments of vortices in the wake of large idealized mountains. *J. Atmos. Sci*., **51**, 191-209.

Sun, W. Y., and W. R. Hsu, 2004: Effect of surface friction on downslope wind and mountain waves (under review).

Sun, W. Y., and W. R. Hsu, 2003. Effect of Surface Condition on Downslope Wind and Mountain waves. International conference on Alpine meteorology and the Mesoscale Alpine Programme meeting 2003. May 19-23, 2003, Brig, Switzerland.